EBioMedicine 20 (2017) 137–149

Contents lists available at ScienceDirect

EBioMedicine

journal homepage: www.ebiomedicine.com

Research Paper

SGLT2 Inhibition by Empagliflozin Promotes Fat Utilization and Browning and Attenuates Inflammation and Insulin Resistance by Polarizing M2 Macrophages in Diet-induced Obese Mice

Liang Xu [a], Naoto Nagata [a], Mayumi Nagashimada [a], Fen Zhuge [a], Yinhua Ni [a], Guanliang Chen [a], Eric Mayoux [b], Shuichi Kaneko [c], Tsuguhito Ota [a,c,*]

[a] Department of Cell Metabolism and Nutrition, Brain/Liver Interface Medicine Research Center, Kanazawa University, Kanazawa, Ishikawa 920-8640, Japan
[b] Boehringer-Ingelheim, Cardio-metabolic Diseases Research, Biberach, Germany
[c] Department of System Biology, Kanazawa University Graduate School of Medical Science, Kanazawa, Ishikawa 920-8640, Japan

ARTICLE INFO

Article history:
Received 18 January 2017
Received in revised form 24 May 2017
Accepted 25 May 2017
Available online 26 May 2017

Keywords:
Sodium glucose cotransporter-2 inhibitor
Obesity
Energy metabolism
Brown adipose tissue
Inflammation
Macrophage

ABSTRACT

Sodium-glucose cotransporter (SGLT) 2 inhibitors increase urinary glucose excretion (UGE), leading to blood glucose reductions and weight loss. However, the impacts of SGLT2 inhibition on energy homeostasis and obesity-induced insulin resistance are less well known. Here, we show that empagliflozin, a SGLT2 inhibitor, enhanced energy expenditure and attenuated inflammation and insulin resistance in high-fat-diet-induced obese (DIO) mice. C57BL/6J mice were pair-fed a high-fat diet (HFD) or a HFD with empagliflozin for 16 weeks. Empagliflozin administration increased UGE in the DIO mice, whereas it suppressed HFD-induced weight gain, insulin resistance, and hepatic steatosis. Moreover, empagliflozin shifted energy metabolism towards fat utilization, elevated AMP-activated protein kinase and acetyl-CoA carbolxylase phosphorylation in skeletal muscle, and increased hepatic and plasma fibroblast growth factor 21 levels. Importantly, empagliflozin increased energy expenditure, heat production, and the expression of uncoupling protein 1 in brown fat and in inguinal and epididymal white adipose tissue (WAT). Furthermore, empagliflozin reduced M1-polarized macrophage accumulation while inducing the anti-inflammatory M2 phenotype of macrophages within WAT and liver, lowering plasma TNFα levels and attenuating obesity-related chronic inflammation. Thus, empagliflozin suppressed weight gain by enhancing fat utilization and browning and attenuated obesity-induced inflammation and insulin resistance by polarizing M2 macrophages in WAT and liver.

1. Introduction

As the global rate of obesity has more than doubled in recent decades, the rates of associated metabolic disorders, including diabetes, non-alcoholic fatty liver disease (NAFLD), and cardiovascular diseases, have also increased markedly. Low-grade sustained inflammation links obesity to insulin resistance and its comorbidities, such as type 2 diabetes and NAFLD (Hotamisligil, 2006; Sell et al., 2012). Excessive fat accumulation increases the infiltration of proinflammatory immune cells into metabolic tissues and causes phenotypic shifts in macrophages, leading to the development of insulin resistance (Lumeng et al., 2007; Weisberg et al., 2003). However, therapeutic approaches for improving systemic energy balance and chronic inflammation in obesity are limited.

Sodium glucose cotransporter-2 (SGLT2) inhibitors have emerged as a promising new class of glucose-lowering drugs for the management of type 2 diabetes. SGLT2 inhibitors increase urinary glucose excretion (UGE), thereby reducing hyperglycaemia and weight with apparent pleiotropic effects (Ferrannini and Solini, 2012; Inzucchi et al., 2015). When large amounts of glucose are forced into urinary excretion processes, whole-body metabolism undergoes adaptive changes involving glucose fluxes, hormonal responses, and fuel selection (Rossetti et al., 1987). Recent clinical studies have shown that the treatment of type 2 diabetes with SGLT2 inhibitors paradoxically increases endogenous

Abbreviations: ALT, Alanine aminotransferase; AMPK, AMP-activated protein kinase; AST, aspartate aminotransferase; ATMs, adipose tissue macrophages; BAT, brown adipose tissue; CT, computed tomographic; DIO, high-fat-diet-induced obese; EGP, endogenous glucose production; Empa, empagliflozin; FACS, fluorescence-activated cell sorting; FGF21, fibroblast growth factor; GTT, glucose tolerance test; H&E, haematoxylin and eosin; HFD, high-fat diet; ITT, insulin tolerance test; LMs, liver macrophages; NAFLD, non-alcoholic fatty liver disease; NASH, non-alcoholic steatohepatitis; NEFA, non-esterified fatty acid; RER, respiratory exchange ratio; SGLT, sodium/glucose cotransporter; TBARS, thiobarbituric acid reactive substances; TC, total cholesterol; TG, triglycerides; UCP1, uncoupling protein 1; UGE, urinary glucose excretion; VO_2, oxygen consumption; VCO_2, carbon dioxide production; WAT, white adipose tissue.

* Corresponding author at: Department of Cell Metabolism and Nutrition, Brain/Liver Interface Medicine Research Center, Kanazawa University, Kanazawa, Ishikawa 920-8640, Japan.
E-mail address: tota@staff.kanazawa-u.ac.jp (T. Ota).

http://dx.doi.org/10.1016/j.ebiom.2017.05.028

glucose production (EGP) despite an overall reduction in fasting hyperglycaemia (Ferrannini et al., 2014; Merovci et al., 2014). Moreover, the chronic administration of empagliflozin drives a fuel shift in which tissue glucose disposal decreases, and lipid use increases (Ferrannini et al., 2016; Ferrannini et al., 2014), although the mechanisms underlying these effects have yet to be determined.

These observations indicate a unique mode of action of SGLT2 inhibitors in which they operate independently of the insulin pathway and yield favourable effects on obesity, ectopic fat accumulation and comorbidities such as insulin resistance and NAFLD. However, the effects of SGLT2 inhibition on energy homeostasis and obesity-associated inflammation remain largely unknown. Therefore, this study aimed to examine the effects of the SGLT2 inhibitor empagliflozin on systemic energy balance and chronic inflammation in high-fat-diet (HFD)-induced obese (DIO) mice.

2. Materials and Methods

2.1. Animals and Diets

Eight-week-old male C57BL/6J mice (Hamamatsu, Japan) were randomly divided into four groups and pair-fed for 16 weeks as follows: (1) normal chow (NC) with 10% of calories from fat (CRF-1, Charles River Laboratories, Wilmington, MA); (2) HFD with 60% of calories from fat (D12492, Research Diets, New Brunswick, NJ); (3) HFD with 0.003% (w/w) empagliflozin (Boehringer Ingelheim Pharma GmbH & Co. KG, Biberach an der Riss, Germany; HFD + Lo Empa, equivalent to 3 mg/kg bodyweight); or (4) HFD with 0.01% (w/w) empagliflozin (HFD + Hi Empa, equivalent to 10 mg/kg bodyweight). All animal procedures were performed in accordance with the standards set forth in the Guidelines for the Care and Use of Laboratory Animals at Kanazawa University, Japan.

2.2. Indirect Calorimetry

After 6 weeks of feeding, the mice were housed individually in indirect calorimeter chambers (Oxymax; Columbus Instruments, Columbus, OH). Calorimetry, daily body weights, and daily food intake data were measured during a 3-day acclimation period followed by a 2-day experimental period. Oxygen consumption (VO_2), carbon dioxide production (VCO_2), and respiratory exchange ratio (RER, VCO_2/VO_2) were evaluated for 2 consecutive days. Energy expenditure was calculated by the formula as energy expenditure $= VO_2 \times [3.815 + (1.232 \times \mathrm{RER})]$ and normalized to the body mass of each subject. Rectal temperature was measured on 3 consecutive days between 9 and 10 am using a microprobe thermometer (Physitemp Instruments, Clifton, NJ).

2.3. Fluorescence-activated Cell Sorting (FACS)

Cells from the liver and epididymal white adipose tissue (eWAT) were prepared as previously described (Kitade et al., 2012; Ni et al., 2015a). The isolated cells were incubated with Fc-Block (BD Bioscience, San Jose, CA), followed by incubation with fluorochrome-conjugated antibodies (Supplementary Table 1). Flow cytometry was performed using a FACSAria II (BD Bioscience), and the data were analysed using the FlowJo software (Tree Star, Ashland, OR).

2.4. Immunohistochemistry

Paraffin-embedded eWAT, liver, and brown adipose tissue (BAT) sections were immunohistochemically stained for F4/80 and uncoupling protein (UCP) 1 as previously described (Brestoff et al., 2015; Zhuge et al., 2016). The quantification of the positive area were calculated by ImageJ software (Version 1.50). The pancreas was stained with anti-insulin and anti-glucagon antibodies (Abcam, Cambridge, UK) followed by secondary antibodies (AlexaFluor 594, AlexaFluor 488; Jackson ImmunoResearch Laboratories, Baltimore, MD) using standard techniques.

2.5. Computed Tomography (CT)

Abdominal fat mass were determined by computed tomography (CT). Briefly, 21-week-old mice ($n = 6$) of each group were scanned by using Latheta LCT-200 (Hitachi-Aloka, Tokyo, Japan) while animals were under 2% isoflurane anaesthesia. Adipose tissue mass in the abdominal region between the proximal end of lumbar vertebra L1 and the distal end of L6 was scanned. And the visceral and subcutaneous fat depots of the area was analysed.

2.6. Biochemical Analyses

Plasma triglycerides (TG), total cholesterol (TC), non-esterified fatty acid (NEFA), glucose, insulin, glucagon, aspartate aminotransferase (AST), alanine aminotransferase (ALT), tumor necrosis factor-α (TNFα), fibroblast growth factor 21 (FGF21), ketone body, glycerol, creatinine and hepatic lipids, ketone body, thiobarbituric acid-reactive substrates (TBARS) concentrations, and urine 8-hydroxy-2′-deoxyguanosine (8-OHdG) contents were measured as described previously (Ni et al., 2015b; Ota et al., 2008).

2.7. GTTs and ITTs

The glucose tolerance test (GTT) was conducted after an overnight fast, and the mice were then injected with 2 g/kg glucose i.p. The insulin tolerance test (ITT) was performed after a 4-h fast, and mice were injected with 1 U/kg human insulin i.p.

2.8. Urinary Glucose Extraction

Mice were housed individually in metabolic cages for 24 h and urine samples were collected and urine volume was measured. Urinary glucose concentration was determined by glucose C2 test kit (Wako Life Sciences, Inc. Osaka, Japan).

2.9. Detection of mRNAs and Proteins

Relative quantification real-time polymerase chain reaction (PCR) and Western blot analyses were performed as described previously (Kitade et al., 2012). Primers used for real-time PCR are shown in Supplementary Table 2, and primary antibodies for Western blotting are shown in Supplementary Table 3.

2.10. Statistics

Results are reported as the means ± SEM. Differences between the mean values were assessed using a two-tailed Student's *t*-test or ANOVA. *P* values <0.05 were considered significant.

3. Results

3.1. Empagliflozin Reduces Weight and Adiposity and Increases UGE in DIO Mice

C57BL/6J mice were pair-fed the NC, HFD, or HFD containing empagliflozin for 16 weeks. The high-dose of empagliflozin suppressed weight gain (Fig. 1a) independently of food intake (Fig. 1b, Supplementary Table 4). However, empagliflozin dose-dependently increased water intake (Fig. 1c). The results from the CT scans showed that abdominal fat accumulation was dose-dependently decreased by empagliflozin in the DIO mice (Fig. 1d, e), and the weights of the visceral and subcutaneous fat depots were consistently decreased by administration of empagliflozin (Fig. 1f). Additionally, the liver and BAT weights

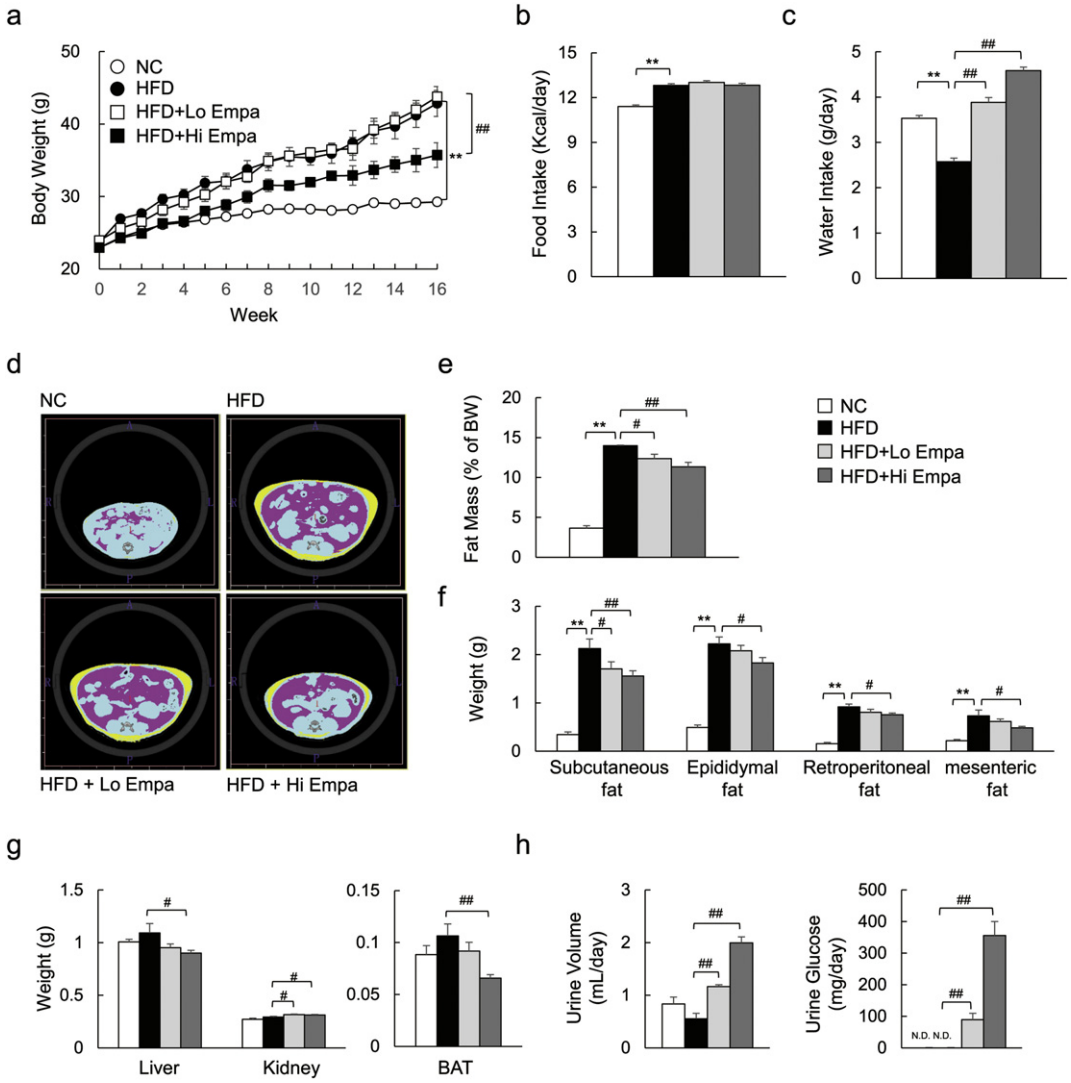

Fig. 1. Empagliflozin reduces weight gain in DIO mice. (a) Body weights. (b, c) Food and water intake. (d) Representative CT images. (e) Fat mass calculated from CT scans. (f, g) Fat depot and tissue weights. (h) Urine volume and urinary glucose. Data are presented as means ± SEM, $n = 7$–9. $^{*}P < 0.05$, $^{**}P < 0.01$ vs. NC; $^{\#}P < 0.05$, $^{\#\#}P < 0.01$ vs. HFD.

were lower in the HFD + Hi Empa group than in the HFD group, whereas the kidney weights increased with both doses of empagliflozin (Fig. 1g). The femoral muscle weight was unaffected by empagliflozin (Supplementary Fig. 1a, b). Moreover, administration of empagliflozin dose-dependently increased urine volume and UGE (Fig. 1h). The genes *Slc5a1* and *Slc5a2*, encoding SGLT1 and SGLT2, respectively, were dose-dependently upregulated in the kidney by empagliflozin (Supplementary Fig. 1c). However, plasma creatinine levels, which are an indicator of renal function, were unaffected by empagliflozin (Supplementary Fig. 1d). Taken together, these data indicate that the weight reduction by empagliflozin was largely attributable to decreases in both visceral and subcutaneous fat depots under pair-fed conditions and that there was no effect on renal function.

3.2. Empagliflozin Ameliorates HFD-induced Insulin Resistance

The high-dose of empagliflozin normalized postprandial hyperglycaemia in the DIO mice (Fig. 2a). The GTT and ITT data showed that glucose intolerance and insulin resistance were ameliorated by empagliflozin (Fig. 2b, c), and hyperinsulinemia in fed and fasting states were suppressed (Fig. 2d). Moreover, the expression levels of *G6pc* and *Pepck*, which are involved in EGP, were elevated by empagliflozin in the DIO mice (Supplementary Fig. 2a). Consistent with these findings, empagliflozin increased fasting glucagon levels (Supplementary Fig. 2b), resulting in a reduced ratio of insulin to glucagon (Fig. 2e). The immunofluorescence analysis revealed that the number and size of the pancreatic islets were increased in the DIO mice, whereas they were dose-dependently decreased by empagliflozin (Fig. 2f, g). Finally, we found the insulin-stimulated phosphorylation of the insulin receptor β subunit (Tyr1146) and Akt (Ser473) in eWAT, liver, and muscle was increased in the HFD + Empa mice compared to the HFD mice (Supplementary Fig. 2c).

3.3. Empagliflozin Increases Energy Expenditure

To assess whole-body energy expenditure, we placed the mice in open-circuit indirect calorimetry cages after 6 weeks of feeding, before an evident change in the body mass of HFD-fed mice was observed. The HFD did not alter VO_2, but it significantly suppressed VCO_2, RER, and energy expenditure (Fig. 3a–d). Empagliflozin-treated mice that were fed the HFD exhibited consistently higher oxygen consumption and tended to exhale more CO_2 than the HFD-fed controls, leading to elevated energy expenditure (Fig. 3a, b, d) although they displayed similar RERs (Fig. 3c). These data suggest that empagliflozin treatment enhances the utilization of both sugar and fat under HFD conditions. Consistent with this increase in energy expenditure, empagliflozin

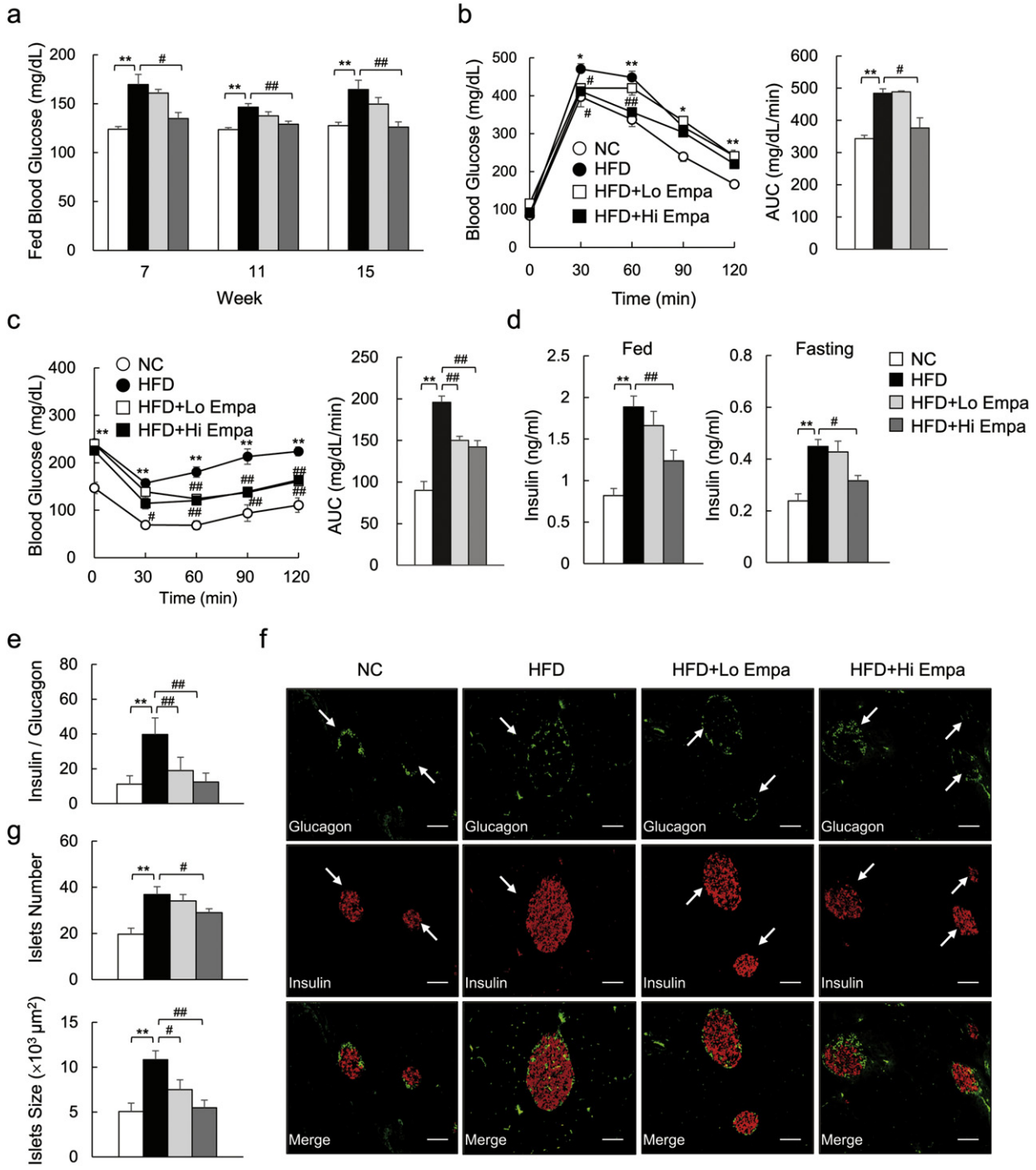

Fig. 2. Empagliflozin ameliorates diet-induced insulin resistance. (a) Fed blood glucose levels. (b, c) GTT and ITT. (d) Plasma insulin levels. (e) Ratio of plasma insulin to glucagon levels. (f) Representative insulin and glucagon-stained pancreas sections. Scale bars = 100 μm. (g) Islet numbers and sizes. Data are presented as means ± SEM, $n = 7$–9. $^{*}P < 0.05$, $^{**}P < 0.01$ vs. NC; $^{\#}P < 0.05$, $^{\#\#}P < 0.01$ vs. HFD.

also increased the core temperature of the mice fed the HFD by ~1 °C (Fig. 3e). These results indicate that empagliflozin reduces obesity by increasing energy expenditure.

3.4. Empagliflozin Promotes the Browning of Fat in DIO Mice

The increased energy expenditure and body temperature of the empagliflozin-treated, HFD-fed mice suggested an increase in adaptive thermogenesis. Indeed, empagliflozin decreased lipid accumulation (Fig. 4a), and increased the number of UCP1^{+} cells in the interscapular BAT (Fig. 4b, Supplementary Fig. 3a). The mRNA levels of brown fat-selective genes were also significantly upregulated by empagliflozin (Fig. 4c). Furthermore, empagliflozin increased UCP1 protein levels in BAT (Fig. 4d). Brown-like adipocytes expressing UCP1, also known as beige cells, exist in various WAT depots and can contribute to thermogenesis (Cohen et al., 2014). The HFD significantly decreased UCP1 protein levels in both eWAT and inguinal WAT (iWAT) compared with NC, and these levels were restored by empagliflozin (Fig. 4d). Consistent with the immunoblotting data, empagliflozin also increased the number of UCP1^{+} cells in both eWAT and iWAT (Supplementary Fig. 3b, c). Additionally, the mRNA levels of beige-selective genes were increased in iWAT (Supplementary Fig. 3d). Thus, empagliflozin appears to promote

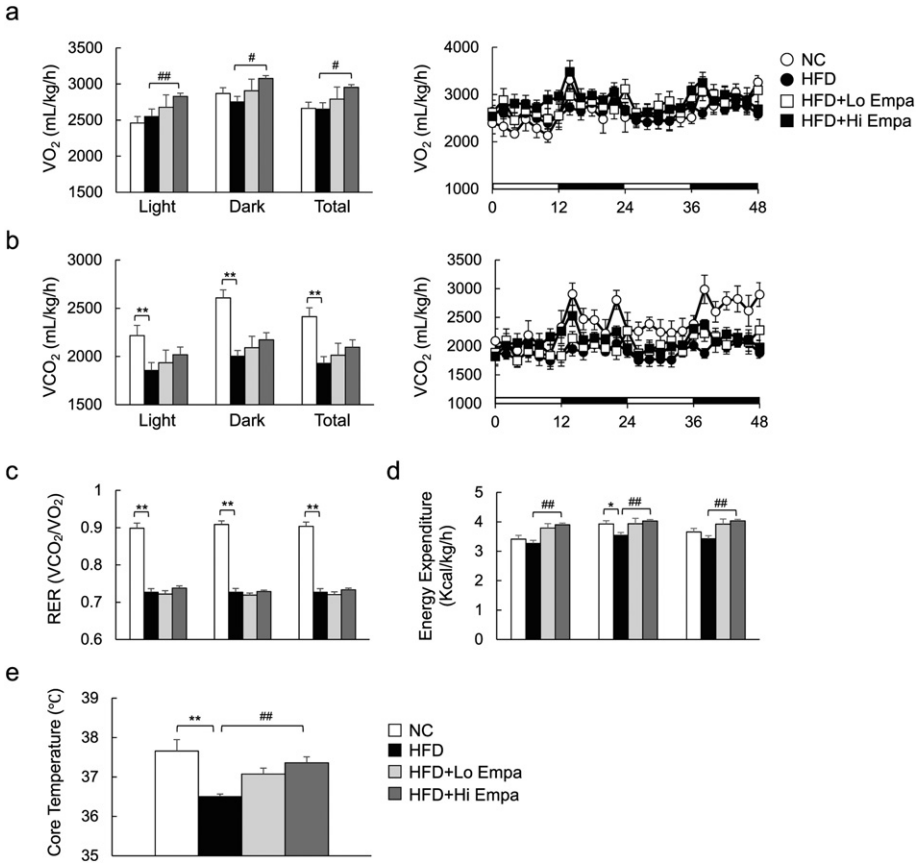

Fig. 3. Empagliflozin increases energy expenditure in DIO mice. (a) Oxygen consumption (VO_2). (b) Carbon dioxide production (VCO_2). (c) Respiratory exchange ratio (RER). (d) Energy expenditure. (e) Rectal temperature. Data are presented as means ± SEM, $n = 7$–9. $^{*}P < 0.05$, $^{**}P < 0.01$ vs. NC; $^{\#}P < 0.05$, $^{\#\#}P < 0.01$ vs. HFD.

fat browning, thereby enhancing energy expenditure in these obese mice.

3.5. Empagliflozin Activates AMP-activated Protein Kinase and Enhances Fatty Acid Oxidation in Skeletal Muscle

Empagliflozin suppressed HFD-induced TG accumulation, associated with the upregulated mRNA expression of fatty acid β-oxidation genes in skeletal muscle (Fig. 5a, b). Furthermore, empagliflozin increased the urinary excretion of ketone bodies and their plasma levels (Fig. 5c). The phosphorylation of AMP-activated protein kinase (AMPKα; at Thr^{172}) and acetyl-CoA carboxylase (ACC; at Ser^{79}) was increased by empagliflozin (Fig. 5d), suggesting that empagliflozin activates AMPK and enhances fat oxidation in skeletal muscle.

3.6. Empagliflozin Attenuates Obesity-induced Inflammation in WAT

We next evaluated the effects of empagliflozin on adipose tissue biology. The mean adipocyte size in eWAT was increased 2.5-fold in the HFD group, and this increase was significantly suppressed by empagliflozin (Fig. 6a, b). The mRNA levels of fatty acid synthesis-related genes were consistently decreased by empagliflozin (Fig. 6d). In contrast, the mRNA levels for of fatty acid β-oxidation-related genes were increased by empagliflozin (Fig. 6d). The obesity-associated aberrant expression of adipokines, such as *leptin* and *adiponectin*, was also improved by empagliflozin (Fig. 6e).

According to the immunostaining and mRNA expression of F4/80, empagliflozin markedly decreased the infiltration of macrophages into the hypertrophic adipose tissue and crown-like structures (Fig. 6a, c, and f), and iWAT (Supplementary Fig. 4a) of the DIO mice. The levels of inflammatory chemokines and cytokines derived from M1 macrophages were decreased in the eWAT of the HFD + Empa mice (Fig. 6f). The plasma levels of TNFα were markedly lower in the HFD + Empa mice than in the HFD mice (Fig. 6g). In contrast, empagliflozin upregulated the mRNA levels of the anti-inflammatory and M2 macrophage markers (Fig. 6h). Empagliflozin also attenuated the phosphorylation of JNK and ERK1/2, although the phosphorylation levels of p38 MAPK and NF-κB p65 were comparable among the treatment groups (Fig. 6i, Supplementary Fig. 4b). Furthermore, the increase in endoplasmic reticulum stress in the DIO mice, as assessed by GRP78 and CHOP protein levels, as well as *spliced XBP1(sXBP1)* and *Grp78* mRNA expression, was suppressed by empagliflozin (Fig. 6i, Supplementary Fig. 4b, c).

The levels of urinary 8-OHdG, a marker of oxidized DNA damage, were increased, but empagliflozin decreased the levels markedly (Fig. 6j). Empagliflozin also suppressed the levels of TBARS, an indicator of lipid peroxidation, in eWAT and plasma by 35.3% and 28.7%, respectively (Fig. 6j). These findings were observed in association with decreased mRNA expression of the subunits of NADPH oxidase (Supplementary Fig. 4d) and increased mRNA expression of anti-oxidative stress genes in the eWAT of the DIO mice (Supplementary Fig. 4e).

3.7. Empagliflozin Protects Mice from Diet-induced Hepatic Steatosis and Inflammation

The histological analysis revealed severe lipid accumulation in the livers of the mice fed the HFD, which was decreased markedly by empagliflozin (Fig. 7a). Empagliflozin consistently reduced the liver TG, TC, and NEFA levels in the HFD-fed mice (Fig. 7b), and these findings were associated with the suppression of lipogenic gene expression and the upregulation of mitochondrial fatty acid β-oxidation genes (Fig. 7c). Moreover, the changes in plasma glycerol levels induced by lipolysis

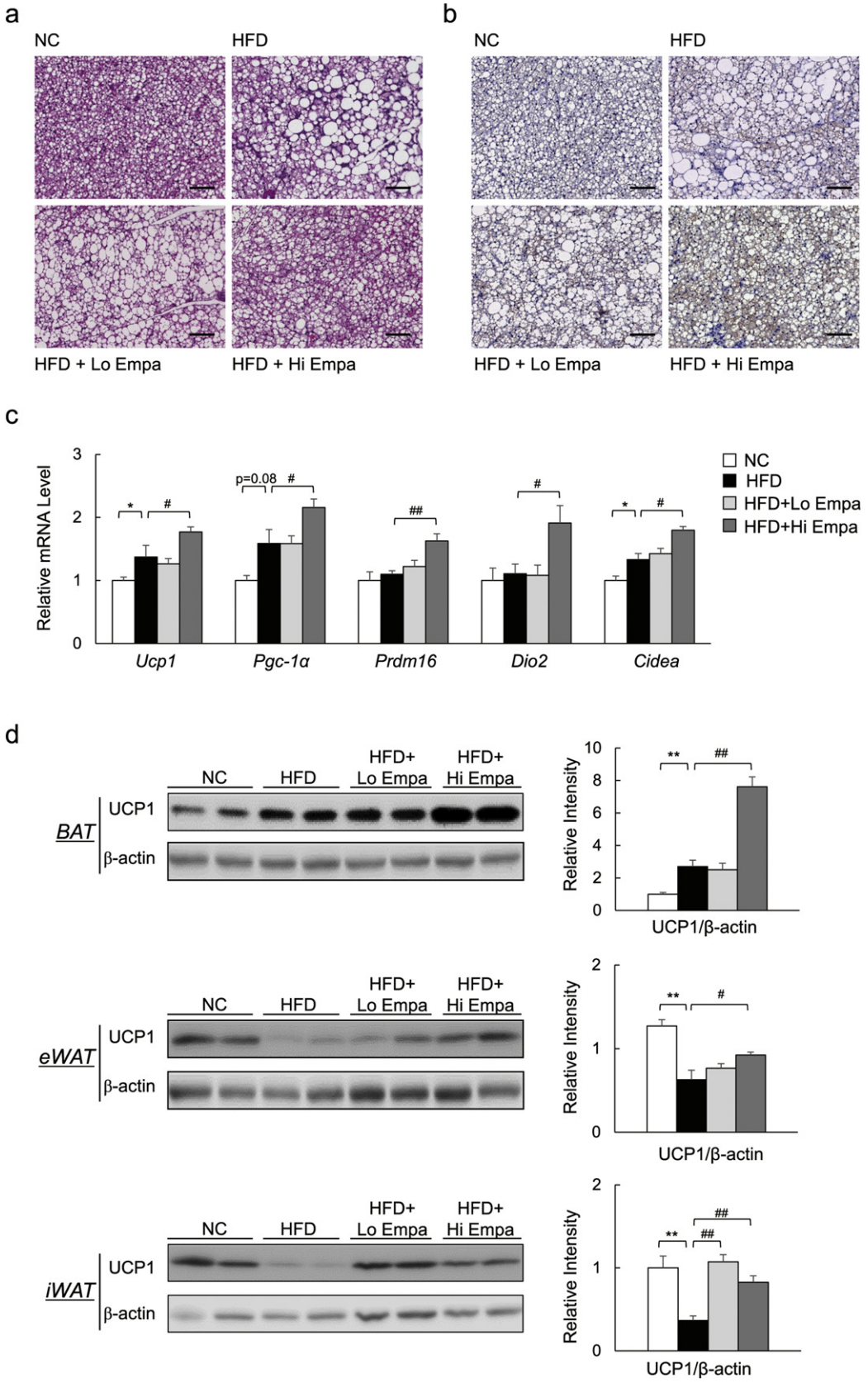

Fig. 4. Empagliflozin increases UCP1 levels in BAT and beige fat. (a) H&E-stained BAT sections. Scale bars = 100 μm. (b) UCP1-stained BAT sections. Scale bars = 100 μm. (c) mRNA expression of brown fat-related genes. (d) Immunobloting and quantitation of UCP1 in BAT, eWAT and iWAT. Data are presented as means ± SEM, $n = 7–9$. $^{*}P < 0.05$, $^{**}P < 0.01$ vs. NC; $^{\#}P < 0.05$, $^{\#\#}P < 0.01$ vs. HFD.

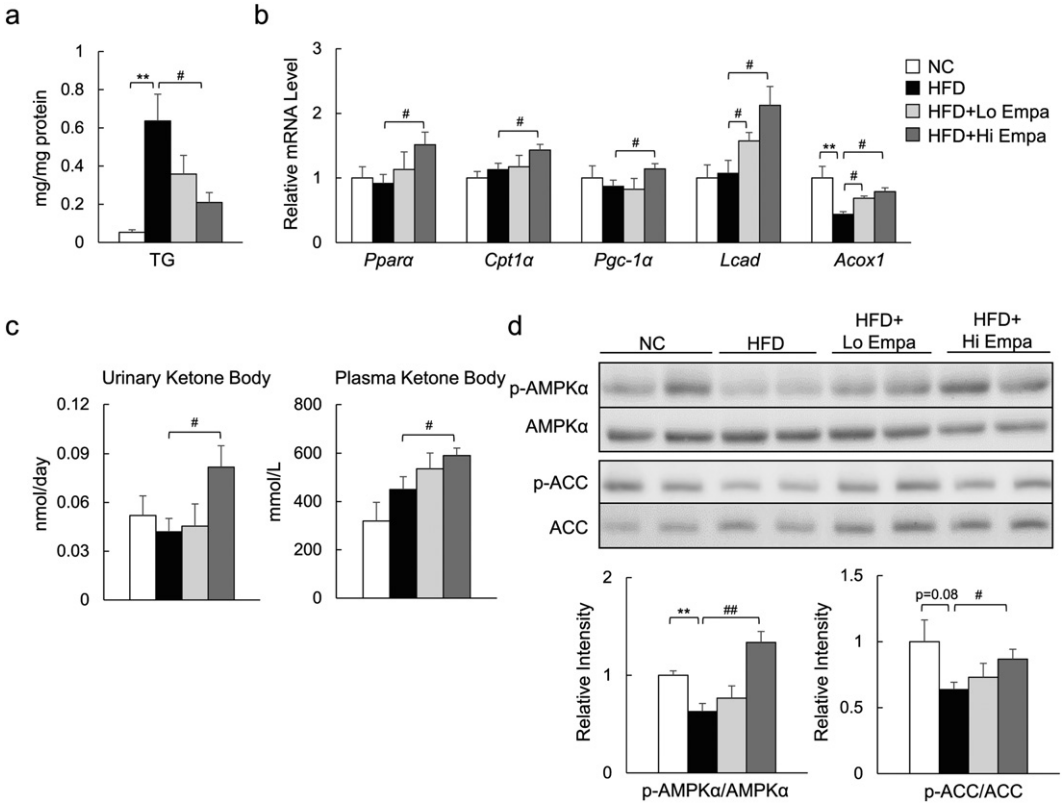

Fig. 5. Empagliflozin enhances fat utilization in skeletal muscle. (a) Muscle TG content. (b) mRNA expression of fatty acid oxidation-related genes. (c) Urinary ketone body and fasting plasma ketone body concentrations. (d) Immunoblotting of skeletal muscle lysates. Data are presented as means ± SEM, $n = 7–9$. $^{*}P < 0.05$, $^{**}P < 0.01$ vs. NC; $^{\#}P < 0.05$, $^{\#\#}P < 0.01$ vs. HFD.

were increased by empagliflozin (Supplementary Table 4). The administration of empagliflozin caused an elevation in the levels of hepatic ketone bodies (Supplementary Fig. 5a) but decreased the levels of plasma AST and ALT; plasma lipid levels were not significantly affected (Supplementary Table 4).

As with WAT, empagliflozin also markedly decreased the number of F4/80^{+} cells (Fig. 7d, e, Supplementary Fig. 5b) and the mRNA expression of proinflammatory cytokines and chemokines in the liver (Fig. 7e), whereas it increased the mRNA levels of anti-inflammatory and M2 macrophage markers (Fig. 7f). These changes were associated with attenuated phosphorylation of NF-κB p65 and JNK and reduced CHOP expression in the liver (Fig. 7g, Supplementary Fig. 5c). Furthermore, the TBARS levels and gene expression of the NADPH oxidase subunits were decreased in the HFD + Empa group compared with the HFD group (Fig. 7h, Supplementary Fig. 5d). However, empagliflozin increased the mRNA levels of anti-oxidative stress genes (Supplementary Fig. 5e). Furthermore, the hepatic mRNA levels of fibroblast growth factor (FGF21) and the plasma levels of FGF21 were increased by empagliflozin in the DIO mice (Fig. 7i). These data suggest that FGF21 can mediate a shift of energy metabolism towards fat utilization in response to SGLT2 inhibition.

3.8. Reciprocal Decreases in M1 Macrophages and Increases in M2 Macrophages in Empagliflozin-fed Mice

To further quantify the adipose tissue macrophages (ATMs) and hepatic macrophage/Kupffer cell subsets, FACS was used to analyse the immune cells isolated from the mice. The increase in the total number of ATMs associated with HFD feeding was decreased slightly by empagliflozin (Fig. 8a, c), and the HFD-fed mice exhibited significantly higher M1 and lower M2 expression levels within the ATMs. The high-dose of empagliflozin caused a 49% decrease in M1 ATMs and a 3.3-fold increase in M2 ATMs compared with HFD feeding, resulting in macrophage polarization towards an anti-inflammatory phenotype (Fig. 8b, c).

Moreover, the total number of liver macrophages (LMs) was increased in the mice fed the HFD compared with the NC diet (Fig. 8d, f). In addition to the reduction in total LM content, the empagliflozin-treated mice had fewer M1 LMs and more M2 LMs than the HFD-fed mice, resulting in macrophage polarization towards an anti-inflammatory phenotype in the liver (Fig. 8e, f). Moreover, the total number of CD3^{+}, CD4^{+}, and CD8^{+} T cells in the eWAT and liver increased with HFD feeding, but this effect was significantly decreased by empagliflozin (Supplementary Fig. 6a–d). These results suggest that empagliflozin causes a shift to an M2-dominant macrophage phenotype and reduces T cell accumulation in the liver and WAT, contributing to the attenuation of obesity-induced insulin resistance and inflammation.

4. Discussion

The present study provides evidence that SGLT2 inhibition is associated with the substantial impacts of empagliflozin on energy homeostasis, obesity-induced inflammation, and insulin resistance. Several studies have demonstrated the protective effects of SGLT2 inhibitors against obesity in rodents. In 8-week-old pair-fed animals, tofogliflozin suppressed HFD-induced weight gain and hepatic steatosis (Obata et al., 2016). In contrast, 4 weeks of treatment with remogliflozin following 11 weeks of HFD feeding attenuated hepatic steatosis without affecting weight gain (Nakano et al., 2015). Another report showed that luseogliflozin decreased liver weight and ameliorated steatohepatitis in streptozotocin-treated mice that were fed a HFD, and it did so without altering weight gain (Qiang et al., 2015). However, the effects of SGLT2 inhibition on energy homeostasis and obesity-related inflammation remain largely unknown. Because SGLT2 inhibitors have been shown to augment food intake in rodents (Devenny et al., 2012; Obata et al., 2016), we pair-fed the mice to clarify the effect of SGLT2 inhibition

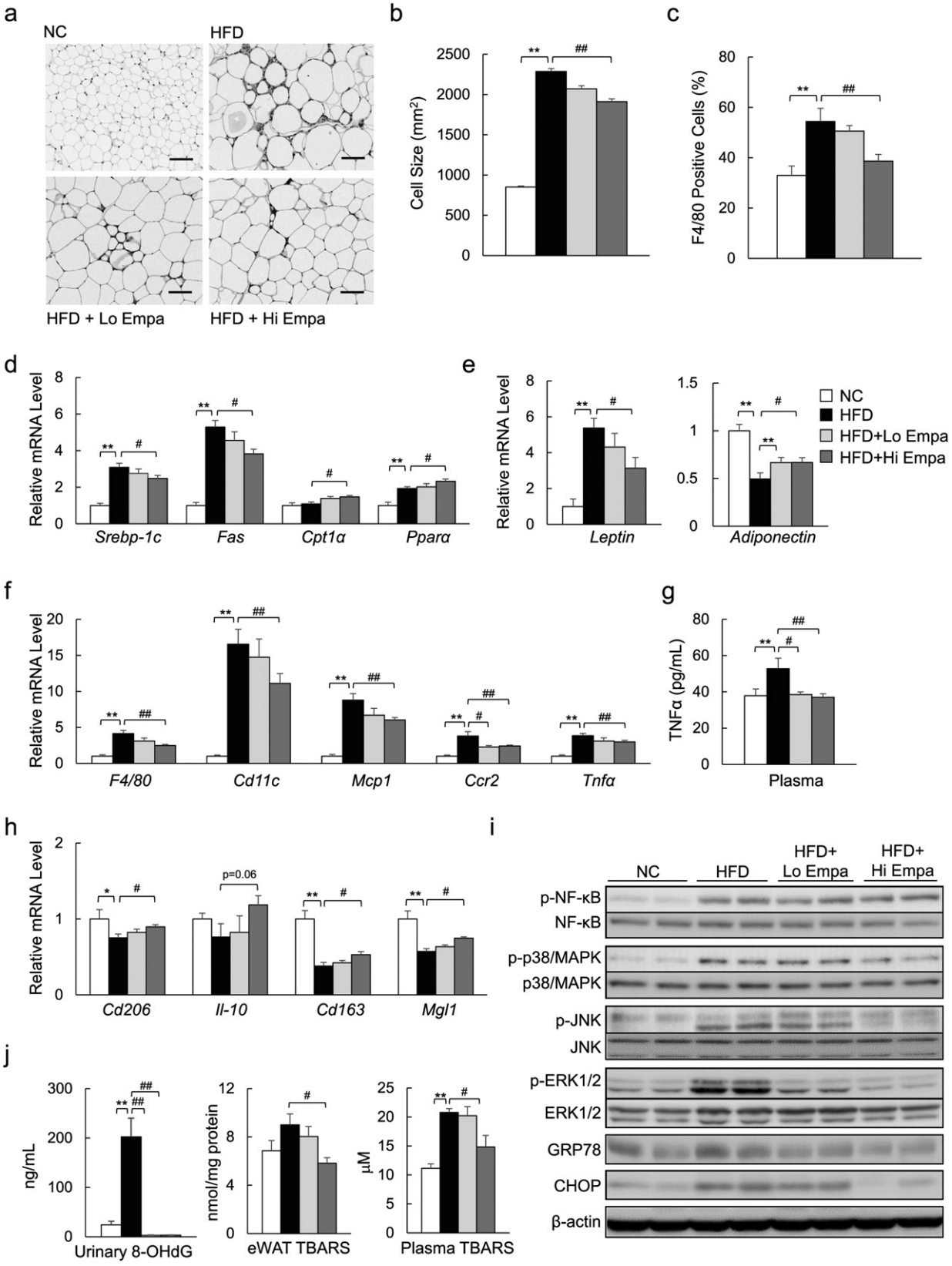

Fig. 6. Empagliflozin attenuates adipose tissue inflammation. (a) F4/80 immunostaining in eWAT. Scale bars = 100 μm. (b) Adipocyte sizes. (c) The F4/80^{+}-cell ratio. (d) mRNA expression of lipometabolic-related genes. (e) mRNA expression of adipocytokine genes. (f) mRNA expression of F4/80 and inflammatory cytokines and chemokines. (g) Plasma levels of TNFα. (h) mRNA expression of M2 marker genes. (i) Immunoblotting of eWAT lysates. (j) Urinary 8-OHdG levels and TBARS content in eWAT and plasma. Data are presented as means ± SEM, $n = 7$–9. $^{*}P < 0.05$, $^{**}P < 0.01$ vs. NC; $^{\#}P < 0.05$, $^{\#\#}P < 0.01$ vs. HFD.

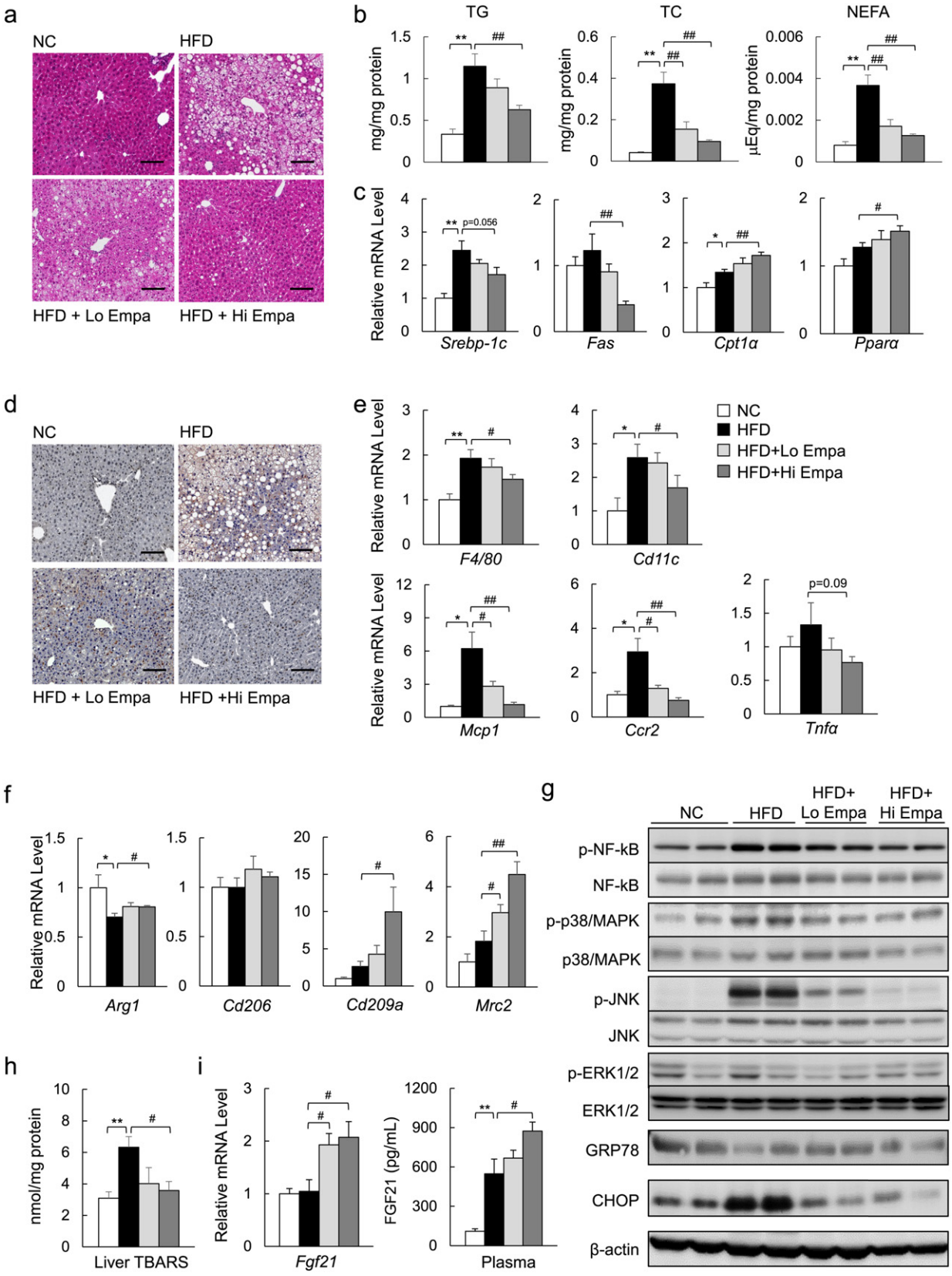

Fig. 7. Empagliflozin ameliorates hepatic steatosis and inflammation. (a) H&E-stained liver sections. Scale bars = 100 μm. (b) Hepatic lipid content. (c) mRNA levels of lipogenic regulator genes. (d) F4/80 immunostaining. Scale bars = 100 μm. (e) mRNA expression of F4/80 and inflammatory cytokines and chemokines. (f) mRNA expression of M2 marker genes. (g) Immunoblotting of liver lysates. (h) TBARS content. (i) mRNA expression of FGF21 in the liver and plasma levels of FGF21. Data are presented as means ± SEM, $n = 7–9$. $^{*}P < 0.05$, $^{**}P < 0.01$ vs. NC; $^{\#}P < 0.05$, $^{\#\#}P < 0.01$ vs. HFD.

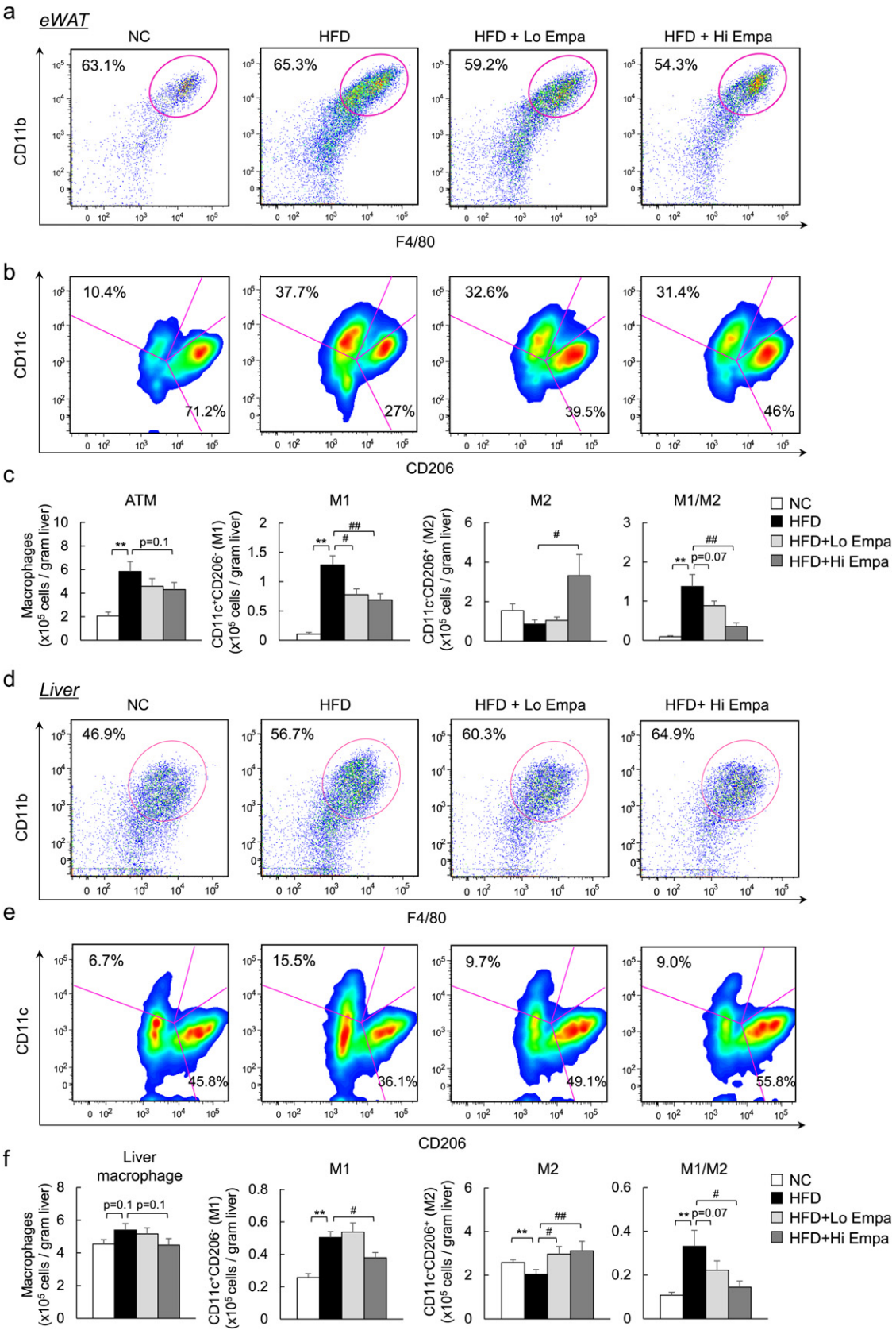

Fig. 8. Empagliflozin treatment leads to a predominance of M2 macrophage populations over M1 in the WAT and liver. (a) Representative plots of total ATMs in eWAT. (b) M1 and M2 macrophages in eWAT. (c) Quantitation of total counts of ATMs, M1 ATMs, and M2 ATMs and M1/M2 ratios. (d) Representative plots of total LMs. (e) M1 and M2 macrophages in the liver. (f) Quantitation of total counts of LMs, M1 LMs, and M2 LMs and M1/M2 ratios. Data are presented as means ± SEM, $n = 7–9$. $^{*}P < 0.05$, $^{**}P < 0.01$ vs. NC; $^{\#}P < 0.05$, $^{\#\#}P < 0.01$ vs. HFD.

on obesity and its comorbidities. Notably, empagliflozin reduced adiposity via increased energy expenditure and caloric loss due to glucosuria. Notable weight loss, particularly in HFD + Hi Empa group, could contribute to the amelioration of obesity-related insulin resistance and metabolic phenotype. The relative expression levels of *Slc5a1* and *Slc5a2* in the kidney were increased, possibly due to a compensatory response to SGLT2 inhibition, as previously reported (Rieg et al., 2014).

Although the present study revealed that increased UGE drove reductions in adiposity and ectopic fat, these findings may be limited because the effects of empagliflozin were evaluated using preventative treatments rather than a therapeutic study design. Additional therapeutic studies will aid in the translation of experimental results regarding the anti-obesity effects of SGLT2 inhibitors to clinical settings. The differences among the clinical doses of empagliflozin used for humans (10 and 25 mg/d) and the experimental doses used for rats (3 mg/kg/d) (Thomas et al., 2012) and mice (3 and 10 mg/kg/d) in the present study may reflect differences in the pharmacokinetic parameters between humans and rodents. The linear pharmacokinetics of empagliflozin indicate that the maximum plasma concentration (C_{max}) after 3 mg/kg of this drug is administered can be estimated as approximately 500 nM; even if a 10-fold higher concentration is assumed to be present in the kidney, this would still be below the apparent Ki (inhibition constant; 8500 nM) of empagliflozin for SGLT-1 (Grempler et al., 2012). Therefore, the relevant inhibition of human, mouse, or rat SGLT-1 by pharmacological doses of empagliflozin would not be expected.

Pharmacologically induced glucosuria leads to adaptive responses in glucose homeostasis and hormone release, and the genetic or pharmacological inhibition of SGLT2 has beneficial effects on hyperinsulinemia and hyperglycaemia (Tahara et al., 2013; Vallon et al., 2013). Conversely, SGLT2 inhibition induces EGP in mice (Bonner et al., 2015; Neschen et al., 2015). In patients with type 2 diabetes, SGLT2 inhibitors also increase EGP and plasma glucagon levels, as well as decrease plasma glucose and insulin levels (Ferrannini et al., 2014; Merovci et al., 2014). The empagliflozin-induced hormonal change in relative hyperglucagonemia can be explained by reductions in glycaemia and insulin release, as insulin normally restrains glucagon secretion via paracrine action (Maruyama et al., 1984). Moreover, a recent study suggested that the inhibition of SGLT2 with dapagliflozin directly triggered glucagon secretion in pancreatic alpha-cells (Bonner et al., 2015). Our study confirmed that empagliflozin induced the expression of genes involved in hepatic glucose production and glucagon release and reduced the ratio of insulin to glucagon. Moreover, empagliflozin decreased the number and size of pancreatic islets, although it did not alter alpha-cell mass. These results suggest that the suppression of hyperinsulinemia by empagliflozin causes relative hyperglucagonemia and increases EGP. This relative hyperglucagonemia may promote lipolysis, contributing to fat utilization and the release of ketone bodies in DIO mice.

Consistent with previous reports demonstrating the anti-obesity effects of SGLT2 inhibitors (Devenny et al., 2012; Nakano et al., 2015; Yokono et al., 2014), we found that the administration of empagliflozin mitigated HFD-induced weight gain and fatty liver changes. Our findings suggest an underlying mechanism for the weight reduction that depends partially on increased energy expenditure and enhanced fatty acid oxidation. In our study, empagliflozin enhances the phosphorylation of AMPKα and ACC in skeletal muscle. A recent study found that canagliflozin activates AMPK in vitro and lowers liver lipid content (Hawley et al., 2016). Once activated, AMPK acts to restore energy homeostasis by promoting catabolic pathways, including fatty acid oxidation, while inhibiting anabolic pathways, including fatty acid synthesis (Hardie, 2014; Hardie et al., 2016). Adiponectin activates AMPK via adiponectin receptor 1 in skeletal muscle (Yamauchi and Kadowaki, 2008). Moreover, the inhibition of SGLT2 increases energy expenditure, leading to the increase of AMP/ATP (Gowans et al., 2013). Therefore, the potential mechanisms of activation of AMPK by empagliflozin are, at least in part, via increased adiponectin expression in WAT and elevation of AMP/ATP. Because the phosphorylation of ACC by AMPK is known to lower muscle lipid content, our results suggest a potential benefit of empagliflozin and other SGLT2 inhibitors in protecting against obesity or ectopic fat accumulation. In the present study, the low dose of empagliflozin tended to increase the phosphorylation levels of ACC and AMPK, which contributed to the decreases in ectopic fat in the liver and muscle in the absence of weight reduction.

An important finding of this study is that empagliflozin increases whole-body energy expenditure, and the protein levels of UCP1 in both BAT and WAT. These data suggest that empagliflozin promotes adipose tissue browning. Recent studies have demonstrated that M2-polarized macrophages play a key role in the browning of WAT via the activation of type 2 cytokine production during cold exposure (Nguyen et al., 2011; Qiu et al., 2014). In response to cold exposure, various cytokines are released from M2-type macrophages; these include catecholamines, which activate β-adrenergic receptors in adipocytes to turn on the thermogenic program, including the induction of UCP1. Moreover, adiponectin plays a role in promoting beige adipocytes (Hui et al., 2015). We found that empagliflozin causes M2 polarization in macrophages and increases adiponectin levels in WAT, which can lead to adipose tissue browning.

FGF21 has emerged as a key mediator of metabolic processes and contributes to the regulation of lipolysis in WAT (Inagaki et al., 2007), and the increase in fatty acid oxidation in the liver (Badman et al., 2007). FGF21 also activates the β_3-adrenergic receptor in WAT and regulates the recruitment of beige adipocytes (Fisher et al., 2012). The systemic administration of FGF21 leads to weight loss in obese mouse models through increases in energy expenditure (Kharitonenkov et al., 2005). Thus, increased FGF21 in the liver and circulation following empagliflozin administration may be another factor promoting fat utilization and browning under the conditions of obesity.

Obesity or ectopic fat accumulation induces an innate immune response with the subsequent recruitment of immune cells, which ultimately leads to the development of insulin resistance and non-alcoholic steatohepatitis (NASH). In particular, macrophage recruitment and polarization are pivotal to obesity-induced inflammation and insulin resistance (Lumeng et al., 2007; Weisberg et al., 2003). Thus, strategies to restrain M1 polarization and/or drive the alternative M2 activation of macrophages may have the potential to protect against exacerbated inflammation and insulin resistance and may even attenuate the progression to NASH (Odegaard et al., 2007; Patsouris et al., 2008; Wan et al., 2014). Our results indicate that empagliflozin attenuates obesity-related inflammation by decreasing macrophage accumulation and causing an M2-dominant phenotypic shift of macrophages in the WAT and liver. Additionally, the infiltration of Th1 and $CD8^+$ T cells precedes M1-polarized macrophage recruitment, and the interactions between the T cells and macrophages constitute a maladaptive feed-forward loop that leads to adipose inflammation and insulin resistance (Nishimura et al., 2009; Sell et al., 2012). Consequently, empagliflozin may reduce the accumulation of T cells and M1 macrophages and increase the amount of M2 macrophages to alleviate inflammation and insulin resistance in obesity. The loss of glucose calories induced by empagliflozin is consistent with increased lipid mobilization, causing a reduction in fat mass and weight (Ferrannini et al., 2016; Ferrannini et al., 2014). Thus, the anti-inflammatory effects of empagliflozin in the WAT and liver may be attributable to its impact on reducing both adiposity and hepatic steatosis.

In conclusion, the present study identified a potential mechanism by which SGLT2 inhibitors reduce obesity and control whole-body energy homeostasis. Empagliflozin-mediated SGLT2 inhibition enhances fat utilization and browning and attenuates obesity-induced inflammation and insulin resistance via M2 or alternative macrophage activation. Overall, the current investigation highlights the potential clinical utility of SGLT2 inhibition in the prevention of obesity and related metabolic disorders, such as insulin resistance, NAFLD, and type 2 diabetes.

Funding

This work was supported by a Grant-in-Aid for Scientific Research (B) (25282017) and for Challenging Exploratory Research (15K12698) from the Ministry of Education, Culture, Sports, Science and Technology of Japan and the Japan Diabetes Foundation (TO).

Duality of Interest

TO received research support from Boehringer Ingelheim Pharma GmbH & Co. KG. No other potential conflict of interest relevant to this article is reported.

Contribution Statement

LX, NN, MN, FZ, YN and GC performed the experiments and gathered the data. EM and SK contributed to discussions. TO contributed to experimental design and wrote the manuscript. All authors approved the final version of the manuscript. TO is responsible for the integrity of the work as a whole.

Acknowledgments

We thank M. Nakayama and K. Hara (Kanazawa University, Kanazawa, Japan) for technical assistance and animal care and AJE for help in the preparation of the manuscript.

Appendix A. Supplementary Data

Supplementary data to this article can be found online at http://dx.doi.org/10.1016/j.ebiom.2017.05.028.

References

Badman, M.K., Pissios, P., Kennedy, A.R., Koukos, G., Flier, J.S., Maratos-Flier, E., 2007. Hepatic fibroblast growth factor 21 is regulated by PPARalpha and is a key mediator of hepatic lipid metabolism in ketotic states. Cell Metab. 5 (6):426–437. http://dx.doi.org/10.1016/j.cmet.2007.05.002.

Bonner, C., Kerr-Conte, J., Gmyr, V., Queniat, G., Moerman, E., Thevenet, J., Beaucamps, C., Delalleau, N., Popescu, I., Malaisse, W.J., et al., 2015. Inhibition of the glucose transporter SGLT2 with dapagliflozin in pancreatic alpha cells triggers glucagon secretion. Nat. Med. 21 (5):512–517. http://dx.doi.org/10.1038/nm.3828.

Brestoff, J.R., Kim, B.S., Saenz, S.A., Stine, R.R., Monticelli, L.A., Sonnenberg, G.F., Thome, J.J., Farber, D.L., Lutfy, K., Seale, P., et al., 2015. Group 2 innate lymphoid cells promote beiging of white adipose tissue and limit obesity. Nature 519 (7542):242–246. http://dx.doi.org/10.1038/nature14115.

Cohen, P., Levy, J.D., Zhang, Y., Frontini, A., Kolodin, D.P., Svensson, K.J., Lo, J.C., Zeng, X., Ye, L., Khandekar, M.J., et al., 2014. Ablation of PRDM16 and beige adipose causes metabolic dysfunction and a subcutaneous to visceral fat switch. Cell 156 (1–2):304–316. http://dx.doi.org/10.1016/j.cell.2013.12.021.

Devenny, J.J., Godonis, H.E., Harvey, S.J., Rooney, S., Cullen, M.J., Pelleymounter, M.A., 2012. Weight loss induced by chronic dapagliflozin treatment is attenuated by compensatory hyperphagia in diet-induced obese (dio) rats. Obesity 20 (8):1645–1652. http://dx.doi.org/10.1038/oby.2012.59.

Ferrannini, E., Solini, A., 2012. SGLT2 inhibition in diabetes mellitus: rationale and clinical prospects. Nat. Rev. Endocrinol. 8 (8):495–502. http://dx.doi.org/10.1038/nrendo.2011.243.

Ferrannini, E., Muscelli, E., Frascerra, S., Baldi, S., Mari, A., Heise, T., Broedl, U.C., Woerle, H.J., 2014. Metabolic response to sodium-glucose cotransporter 2 inhibition in type 2 diabetic patients. J. Clin. Invest. 124 (2):499–508. http://dx.doi.org/10.1172/JCI72227.

Ferrannini, E., Baldi, S., Frascerra, S., Astiarraga, B., Heise, T., Bizzotto, R., Mari, A., Pieber, T.R., Muscelli, E., 2016. Shift to fatty substrate utilization in response to sodium-glucose votransporter 2 inhibition in subjects without diabetes and patients with type 2 diabetes. Diabetes 65 (5):1190–1195. http://dx.doi.org/10.2337/db15-1356.

Fisher, F.M., Kleiner, S., Douris, N., Fox, E.C., Mepani, R.J., Verdeguer, F., Wu, J., Kharitonenkov, A., Flier, J.S., Maratos-Flier, E., et al., 2012. FGF21 regulates pgc-1alpha and browning of white adipose tissues in adaptive thermogenesis. Genes Dev. 26 (3):271–281. http://dx.doi.org/10.1101/gad.177857.111.

Gowans, G.J., Hawley, S.A., Ross, F.A., Hardie, D.G., 2013. Amp is a true physiological regulator of amp-activated protein kinase by both allosteric activation and enhancing net phosphorylation. Cell Metab. 18 (4):556–566. http://dx.doi.org/10.1016/j.cmet.2013.08.019.

Grempler, R., Thomas, L., Eckhardt, M., Himmelsbach, F., Sauer, A., Sharp, D.E., Bakker, R.A., Mark, M., Klein, T., Eickelmann, P., 2012. Empagliflozin, a novel selective sodium glucose cotransporter-2 (SGLT-2) inhibitor: characterisation and comparison with other SGLT-2 inhibitors. Diabetes Obes. Metab. 14 (1):83–90. http://dx.doi.org/10.1111/j.1463-1326.2011.01517.x.

Hardie, D.G., 2014. AMPK-sensing energy while talking to other signaling pathways. Cell Metab. 20 (6):939–952. http://dx.doi.org/10.1016/j.cmet.2014.09.013.

Hardie, D.G., Schaffer, B.E., Brunet, A., 2016. AMPK: an energy-sensing pathway with multiple inputs and outputs. Trends Cell Biol. 26 (3):190–201. http://dx.doi.org/10.1016/j.tcb.2015.10.013.

Hawley, S.A., Ford, R.J., Smith, B.K., Gowans, G.J., Mancini, S.J., Pitt, R.D., Day, E.A., Salt, I.P., Steinberg, G.R., Hardie, D.G., 2016. The Na^+/glucose co-transporter inhibitor canagliflozin activates AMP-activated protein kinase by inhibiting mitochondrial function and increasing cellular AMP levels. Diabetes 65 (9):2784–2794. http://dx.doi.org/10.2337/db16-0058.

Hotamisligil, G.S., 2006. Inflammation and metabolic disorders. Nature 444 (7121):860–867. http://dx.doi.org/10.1038/nature05485.

Hui, X., Gu, P., Zhang, J., Nie, T., Pan, Y., Wu, D., Feng, T., Zhong, C., Wang, Y., Lam, K.S., et al., 2015. Adiponectin enhances cold-induced browning of subcutaneous adipose tissue via promoting M2 macrophage proliferation. Cell Metab. 22 (2):279–290. http://dx.doi.org/10.1016/j.cmet.2015.06.004.

Inagaki, T., Dutchak, P., Zhao, G., Ding, X., Gautron, L., Parameswara, V., Li, Y., Goetz, R., Mohammadi, M., Esser, V., et al., 2007. Endocrine regulation of the fasting response by pparalpha-mediated induction of fibroblast growth factor 21. Cell Metab. 5 (6):415–425. http://dx.doi.org/10.1016/j.cmet.2007.05.003.

Inzucchi, S.E., Zinman, B., Wanner, C., Ferrari, R., Fitchett, D., Hantel, S., Espadero, R.M., Woerle, H.J., Broedl, U.C., Johansen, O.E., 2015. SGLT-2 inhibitors and cardiovascular risk: proposed pathways and review of ongoing outcome trials. Diab. Vasc. Dis. Res. 12 (2):90–100. http://dx.doi.org/10.1177/1479164114559852.

Kharitonenkov, A., Shiyanova, T.L., Koester, A., Ford, A.M., Micanovic, R., Galbreath, E.J., Sandusky, G.E., Hammond, L.J., Moyers, J.S., Owens, R.A., et al., 2005. FGF-21 as a novel metabolic regulator. J. Clin. Invest. 115 (6):1627–1635. http://dx.doi.org/10.1172/JCI23606.

Kitade, H., Sawamoto, K., Nagashimada, M., Inoue, H., Yamamoto, Y., Sai, Y., Takamura, T., Yamamoto, H., Miyamoto, K., Ginsberg, H.N., et al., 2012. CCR5 plays a critical role in obesity-induced adipose tissue inflammation and insulin resistance by regulating both macrophage recruitment and M1/M2 status. Diabetes 61 (7):1680–1690. http://dx.doi.org/10.2337/db11-1506/-/DC1.

Lumeng, C.N., Bodzin, J.L., Saltiel, A.R., 2007. Obesity induces a phenotypic switch in adipose tissue macrophage polarization. J. Clin. Invest. 117 (1):175–184. http://dx.doi.org/10.1172/JCI29881.

Maruyama, H., Hisatomi, A., Orci, L., Grodsky, G.M., Unger, R.H., 1984. Insulin within islets is a physiologic glucagon release inhibitor. J. Clin. Invest. 74 (6):2296–2299. http://dx.doi.org/10.1172/JCI111658.

Merovci, A., Solis-Herrera, C., Daniele, G., Eldor, R., Fiorentino, T.V., Tripathy, D., Xiong, J., Perez, Z., Norton, L., Abdul-Ghani, M.A., et al., 2014. Dapagliflozin improves muscle insulin sensitivity but enhances endogenous glucose production. J. Clin. Invest. 124 (2):509–514. http://dx.doi.org/10.1172/JCI70704.

Nakano, S., Katsuno, K., Isaji, M., Nagasawa, T., Buehrer, B., Walker, S., Wilkison, W.O., Cheatham, B., 2015. Remogliflozin etabonate improves fatty liver disease in diet-induced obese male mice. J. Clin. Exp. Hepatol. 5 (3):190–198. http://dx.doi.org/10.1016/j.jceh.2015.02.005.

Neschen, S., Scheerer, M., Seelig, A., Huypens, P., Schultheiss, J., Wu, M., Wurst, W., Rathkolb, B., Suhre, K., Wolf, E., et al., 2015. Metformin supports the antidiabetic effect of a sodium glucose cotransporter 2 inhibitor by suppressing endogenous glucose production in diabetic mice. Diabetes 64 (1):284–290. http://dx.doi.org/10.2337/db14-0393.

Nguyen, K.D., Qiu, Y., Cui, X., Goh, Y.P., Mwangi, J., David, T., Mukundan, L., Brombacher, F., Locksley, R.M., Chawla, A., 2011. Alternatively activated macrophages produce catecholamines to sustain adaptive thermogenesis. Nature 480 (7375):104–108. http://dx.doi.org/10.1038/nature10653.

Ni, Y., Nagashimada, M., Zhan, L., Nagata, N., Kobori, M., Sugiura, M., Ogawa, K., Kaneko, S., Ota, T., 2015a. Prevention and reversal of lipotoxicity-induced hepatic insulin resistance and steatohepatitis in mice by an antioxidant carotenoid, beta-cryptoxanthin. Endocrinology 156 (3):987–999. http://dx.doi.org/10.1210/en.2014-1776.

Ni, Y., Nagashimada, M., Zhuge, F., Zhan, L., Nagata, N., Tsutsui, A., Nakanuma, Y., Kaneko, S., Ota, T., 2015b. Astaxanthin prevents and reverses diet-induced insulin resistance and steatohepatitis in mice: a comparison with vitamin e. Sci. Rep. 5:17192. http://dx.doi.org/10.1038/srep17192.

Nishimura, S., Manabe, I., Nagasaki, M., Eto, K., Yamashita, H., Ohsugi, M., Otsu, M., Hara, K., Ueki, K., Sugiura, S., et al., 2009. CD8+ effector t cells contribute to macrophage recruitment and adipose tissue inflammation in obesity. Nat. Med. 15 (8):914–920. http://dx.doi.org/10.1038/nm.1964.

Obata, A., Kubota, N., Kubota, T., Iwamoto, M., Sato, H., Sakurai, Y., Takamoto, I., Katsuyama, H., Suzuki, Y., Fukazawa, M., et al., 2016. Tofogliflozin improves insulin resistance in skeletal muscle and accelerates lipolysis in adipose tissue in male mice. Endocrinology 157 (3):1029–1042. http://dx.doi.org/10.1210/en.2015-1588.

Odegaard, J.I., Ricardo-Gonzalez, R.R., Goforth, M.H., Morel, C.R., Subramanian, V., Mukundan, L., Eagle, A.R., Vats, D., Brombacher, F., Ferrante, A.W., et al., 2007. Macrophage-specific ppargamma controls alternative activation and improves insulin resistance. Nature 447 (7148):1116–1120. http://dx.doi.org/10.1038/nature05894.

Ota, T., Gayet, C., Ginsberg, H.N., 2008. Inhibition of apolipoprotein B100 secretion by lipid-induced hepatic endoplasmic reticulum stress in rodents. J. Clin. Invest. 118 (1):316–332. http://dx.doi.org/10.1172/JCI32752.

Patsouris, D., Li, P.P., Thapar, D., Chapman, J., Olefsky, J.M., Neels, J.G., 2008. Ablation of CD11c-positive cells normalizes insulin sensitivity in obese insulin resistant animals. Cell Metab. 8 (4):301–309. http://dx.doi.org/10.1016/j.cmet.2008.08.015.

Qiang, S., Nakatsu, Y., Seno, Y., Fujishiro, M., Sakoda, H., Kushiyama, A., Mori, K., Matsunaga, Y., Yamamotoya, T., Kamata, H., et al., 2015. Treatment with the SGLT2 inhibitor luseogliflozin improves nonalcoholic steatohepatitis in a rodent model with diabetes mellitus. Diabetol. Metab. Syndr. 7:104. http://dx.doi.org/10.1186/s13098-015-0102-8.

Qiu, Y., Nguyen, K.D., Odegaard, J.I., Cui, X., Tian, X., Locksley, R.M., Palmiter, R.D., Chawla, A., 2014. Eosinophils and type 2 cytokine signaling in macrophages orchestrate development of functional beige fat. Cell 157 (6):1292–1308. http://dx.doi.org/10.1016/j.cell.2014.03.066.

Rieg, T., Masuda, T., Gerasimova, M., Mayoux, E., Platt, K., Powell, D.R., Thomson, S.C., Koepsell, H., Vallon, V., 2014. Increase in SGLT1-mediated transport explains renal glucose reabsorption during genetic and pharmacological SGLT2 inhibition in euglycemia. Am. J. Physiol. Renal Physiol. 306 (2):F188–F193. http://dx.doi.org/10.1152/ajprenal.00518.2013.

Rossetti, L., Smith, D., Shulman, G.I., Papachristou, D., DeFronzo, R.A., 1987. Correction of hyperglycemia with phlorizin normalizes tissue sensitivity to insulin in diabetic rats. J. Clin. Invest. 79 (5):1510–1515. http://dx.doi.org/10.1172/JCI112981.

Sell, H., Habich, C., Eckel, J., 2012. Adaptive immunity in obesity and insulin resistance. Nat. Rev. Endocrinol. 8 (12):709–716. http://dx.doi.org/10.1038/nrendo.2012.114.

Tahara, A., Kurosaki, E., Yokono, M., Yamajuku, D., Kihara, R., Hayashizaki, Y., Takasu, T., Imamura, M., Li, Q., Tomiyama, H., et al., 2013. Effects of SGLT2 selective inhibitor ipragliflozin on hyperglycemia, hyperlipidemia, hepatic steatosis, oxidative stress, inflammation, and obesity in type 2 diabetic mice. Eur. J. Pharmacol. 715 (1–3): 246–255. http://dx.doi.org/10.1016/j.ejphar.2013.05.014.

Thomas, L., Grempler, R., Eckhardt, M., Himmelsbach, F., Sauer, A., Klein, T., Eickelmann, P., Mark, M., 2012. Long-term treatment with empagliflozin, a novel, potent and selective SGLT-2 inhibitor, improves glycaemic control and features of metabolic syndrome in diabetic rats. Diabetes Obes. Metab. 14 (1):94–96. http://dx.doi.org/10.1111/j.1463-1326.2011.01518.x.

Vallon, V., Rose, M., Gerasimova, M., Satriano, J., Platt, K.A., Koepsell, H., Cunard, R., Sharma, K., Thomson, S.C., Rieg, T., 2013. Knockout of Na-glucose transporter SGLT2 attenuates hyperglycemia and glomerular hyperfiltration but not kidney growth or injury in diabetes mellitus. Am. J. Physiol. Renal Physiol. 304 (2):F156–F167. http://dx.doi.org/10.1152/ajprenal.00409.2012.

Wan, J., Benkdane, M., Teixeira-Clerc, F., Bonnafous, S., Louvet, A., Lafdil, F., Pecker, F., Tran, A., Gual, P., Mallat, A., et al., 2014. M2 kupffer cells promote M1 kupffer cell apoptosis: a protective mechanism against alcoholic and nonalcoholic fatty liver disease. Hepatology 59 (1):130–142. http://dx.doi.org/10.1002/hep.26607.

Weisberg, S.P., McCann, D., Desai, M., Rosenbaum, M., Leibel, R.L., Ferrante Jr., A.W., 2003. Obesity is associated with macrophage accumulation in adipose tissue. J. Clin. Invest. 112 (12):1796–1808. http://dx.doi.org/10.1172/JCI19246.

Yamauchi, T., Kadowaki, T., 2008. Physiological and pathophysiological roles of adiponectin and adiponectin receptors in the integrated regulation of metabolic and cardiovascular diseases. Int. J. Obes. 32 (Suppl. 7):S13–S18. http://dx.doi.org/10.1038/ijo.2008.233.

Yokono, M., Takasu, T., Hayashizaki, Y., Mitsuoka, K., Kihara, R., Muramatsu, Y., Miyoshi, S., Tahara, A., Kurosaki, E., Li, Q., et al., 2014. SGLT2 selective inhibitor ipragliflozin reduces body fat mass by increasing fatty acid oxidation in high-fat diet-induced obese rats. Eur. J. Pharmacol. 727:66–74. http://dx.doi.org/10.1016/j.ejphar.2014.01.040.

Zhuge, F., Ni, Y., Nagashimada, M., Nagata, N., Xu, L., Mukaida, N., Kaneko, S., Ota, T., 2016. DPP-4 inhibition by linagliptin attenuates obesity-related inflammation and insulin resistance by regulating M1/M2 macrophage polarization. Diabetes 65 (10): 2966–2979. http://dx.doi.org/10.2337/db16-0317.